

# Effect of Spacer Chemistry on the Formation and Properties of Linear Reversible Polymers

James D. Mayo,<sup>1</sup> Alex Adronov<sup>2</sup>

<sup>1</sup>Xerox Research Centre of Canada, 2660 Speakman Drive, Mississauga, Ontario, Canada L5K 2L1

<sup>2</sup>McMaster University, Department of Chemistry, 1280 Main Street West, Hamilton, Ontario, Canada L8S 4L8

Correspondence to: A. Adronov (E-mail: adronov@mcmaster.ca)

Received 22 July 2013; accepted 29 August 2013; published online 25 September 2013

DOI: 10.1002/pola.26937

**ABSTRACT:** A series of four pairs of bismaleimide and bisfuran monomers were combined to make thermally reversible linear polymers. The monomers were prepared using diamines having different spacer chemistries, *n*-octyl, cyclohexyl, phenyl, and ethylenedioxy, such that a relatively constant spacer dimension among the four monomers was achieved. Heating of the bismaleimide/bisfuran couples resulted in low-viscosity, easily processable liquids. Subsequent cooling to room temperature resulted in the formation of hard films, with the rate of hardening varying significantly within the series of compounds. The rate and degree of polymerization were deter-

mined using <sup>1</sup>H NMR spectroscopy and were both found to be dependent on the chemistry of the spacer group, as was the film rheology, which was measured using nanoindentation. Adhesion of the polymers was quantified by measurement of their tensile adhesive strength, and this was also found to be spacer dependent. Polymerization reversibility was verified using <sup>1</sup>H NMR spectroscopy. © 2013 Wiley Periodicals, Inc. *J. Polym. Sci., Part A: Polym. Chem.* **2013**, *51*, 5056–5066

**KEYWORDS:** Diels-Alder polymers; rheology; step-growth polymerization; structure–property relations; synthesis

**INTRODUCTION** Reversible polymers have been explored as a potential solution for thermal and mechanical breakdown of both structural and thin film polymers in a variety of applications.<sup>1–5</sup> Formation and propagation of microcracks within a polymer matrix ultimately led to failure of the material. Reparation using traditional adhesive-based methods only occurs on a macroscale and does not treat the fracture at its onset. With reversible polymers, reparation can occur on a nanoscale within the crack and can be implemented well before it has propagated to the point of material failure. The inherent low viscosity of the monomeric materials enables flow and realignment of the reactive sites across the damaged area, allowing formation of covalent bonds across the microcrack without the use of healing agents or additives. This in turn enables much higher healing efficiencies than have been realized with traditional epoxies or surface treatments and also allows the material to undergo multiple healing events.<sup>6–10</sup> The basic concept for reversible polymers, as depicted in Figure 1, has been explored by numerous investigators using both covalent and noncovalent bonding motifs. In the molten state, reversible polymers can consist of discrete, small molecule building blocks<sup>8–10</sup> [Fig. 1(a)] or of linear polymers that have been decorated with reversible functional groups [Fig. 1(b)].<sup>11–15</sup> The reversible

bonds can therefore be used either to intrinsically generate a polymer network or to impart crosslinking to existing chains. In either case, the viscosity of the heated material would be expected to be significantly lower than would be realized by heating an analogous conventional polymer. These materials therefore not only lend themselves to the concept of self-healing but also allow for much easier materials processing than their polymeric counterparts.

Ideally, the linking chemistry in a reversible polymer is based on an addition rather than a condensation reaction, as the latter would result in liberation of small molecules that would render the reaction irreversible. The Diels-Alder (DA) reaction meets this requirement and has been studied extensively as a reversible coupling method. In particular, the coupling of maleimides and furans has been the basis of much of the work in this field, as the electron-deficient dienophile and *s*-cis-configured diene are ideally suited for reversible DA chemistry.<sup>6–10,16</sup> This system was explored by Wudl and coworkers,<sup>10</sup> who prepared reversible, cross-linked polymers using multivalent maleimides and furans. In their work, a tetrapodal furan and tripodal maleimide were polymerized via DA cycloaddition to form tough, crosslinked polymers that could be reversibly melted and

Additional Supporting Information may be found in the online version of this article.

© 2013 Wiley Periodicals, Inc.

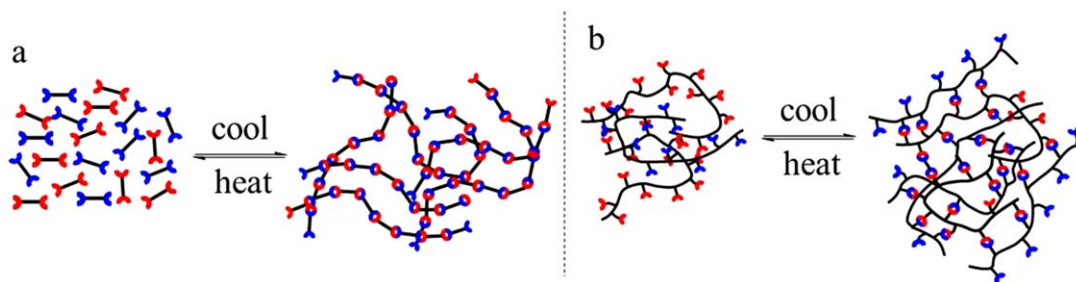


**FIGURE 1** Schematic representation of reversible polymer formation (a) monomeric components and (b) decorated polymer backbone. [Color figure can be viewed in the online issue, which is available at [wileyonlinelibrary.com](http://wileyonlinelibrary.com).]

solidified (Fig. 2). Tensile and compression strength and moduli were measured and compared favorably with typical epoxy resins. The practicality of this phenomenon was then demonstrated by repeated restoration of a fractured polymer via multiple heating and cooling cycles. A novel method of inducing and repairing cracks in the materials was used to quantify healing efficiency; by ensuring close alignment of the two newly exposed surfaces during the repair, the polymers were found to recover more than 80% of their original strength. Further exploration by this group resulted in several remendable crosslinked polymeric materials that were also able to undergo multiple healing events.<sup>9</sup>

Along similar lines, decoration of existing polymer backbones with reactive furan groups was explored by Zhang et al.<sup>15</sup> using readily available polyketones, which were converted to furan derivatives using mild conditions in a Paal-Knorr reaction with furfurylamine. A bisphenyl-based bismaleimide was then used as a crosslinking agent to afford a healable epoxy resin. Healing efficiencies of 100% were reported; however, in this case, healing was measured by grinding the entire sample of solidified resin into a powder and remolding a fresh sample for a repeat mechanical analysis measurement.

Murphy et al.<sup>17</sup> improved on the maleimide–furan coupling, as they prepared a single component remendable polymer using dicyclopentadiene as both diene and dienophile. This linkage was used to form macrocyclic “mendomers,” which,

on heating, would undergo ring opening via the retro DA reaction. The resulting bis(cyclopentadiene) could then couple intermolecularly to form linear reversible polymers. Indeed, this resulted in transparent, hard polymers that could be healed multiple times. A significant amount of additional work has been done to improve the DA reaction, including optimization of the temperature required to induce the retro-DA reaction<sup>18</sup> and variation of the DA reaction rate by modifying the electronics of the diene and dienophile.<sup>19</sup> In addition to the DA reaction, other reversible polymerizations have been investigated for self-healing materials, including carbene dimerization,<sup>20,21</sup> photochemical cycloadditions,<sup>22,23</sup> hydrogen bonding,<sup>24–26</sup> and transesterification.<sup>27</sup>

Although crosslinking offers the opportunity for formation of structurally durable materials, and much of the research in the field of reversible polymers is based on multipodal furans and maleimides that result in highly crosslinked networks, the resulting structures are complex and difficult to characterize. Linear polymers, composed of bismaleimides and bisfurans with different spacer compositions, have received less attention.<sup>28–30</sup> Here, we study the effects of the spacer chemistries on the reaction kinetics and physical properties of the cured polymers. Initially, a relatively simple system consisting of short-chain bisfurans/bismaleimides was chosen to observe the effects of reversible polymerization on overall rheological characteristics, as well as the extent of the coupling reaction. To this end, four different spacer groups were used, including a straight chain alkyl (C<sub>8</sub>), a cyclohexyl, a phenyl, and an ethylenedioxy group.

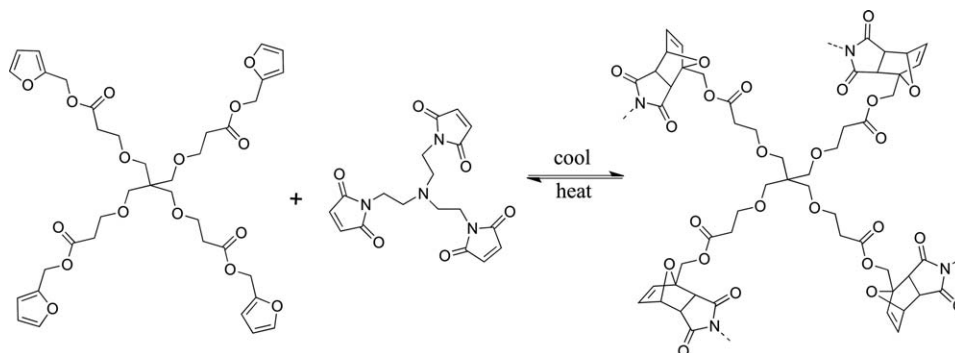


**FIGURE 2** Preparation of crosslinked reversible polymer by Diels-Alder chemistry.

**EXPERIMENTAL****General**

All reagents were obtained from Sigma-Aldrich and used as received.  $^1\text{H}$  NMR spectra were obtained on a Bruker Avance 400-MHz spectrometer using deuterated dimethyl sulfoxide ( $d_6$ -DMSO) as solvent and tetramethylsilane as internal reference. Viscosity measurements were made using an Ares 2000 viscometer obtained from Rheometric Scientific, equipped with a 25-mm steel plate assembly set at a gap width of 200  $\mu\text{m}$ . Nanoindentation measurements were made using a Hysitron Triboscan<sup>®</sup> nanoindenter equipped with a Berkovich diamond tip. Differential scanning calorimetry (DSC) analyses were performed on a DSC Q1000 obtained from TA Instruments. X-ray diffraction (XRD) spectra were obtained on a Rigaku MiniFlex X-ray diffractometer, fitted with a Cu target and variable slit interlocked with  $\theta$  axis. High-resolution mass spectrometry using electrospray ionization was conducted for the synthesized monomers on a Micromass Quattro Ultima triple quadrupole mass spectrometer using positive ion mode. Tensile strength measurements were made on an Instron 3367, using an extension rate of 100  $\mu\text{m}/\text{min}$ .

**General Procedure for Synthesis of Bismaleimides**

To a 500-mL round-bottomed flask equipped with a magnetic stir bar, maleic anhydride (10.5 equiv) in 75 mL DMF was dissolved. The resulting solution was chilled on ice, and the 1,8-octanediamine (5 equiv) dissolved in DMF (75 mL) was added dropwise over  $\sim 20$  min. The ice bath was removed, and sodium acetate (1 equiv) and acetic anhydride (11 equiv) were added in one portion, and then the mixture was stirred overnight at 50  $^\circ\text{C}$ . The mixture turned dark brown within 30 min of the addition of NaOAc and  $\text{Ac}_2\text{O}$ . DMF was removed by vacuum distillation (60  $^\circ\text{C}$ ), and dichloromethane (DCM, 150 mL) was added to the dark brown mixture. The organic layer was extracted with  $\text{NaHCO}_3$  ( $5 \times 100$  mL) and dried over  $\text{MgSO}_4$ , and the solvent was removed under vacuum. The resulting compounds were purified by column chromatography.

**1,1'-(Octane-1,8-diyl)bis(1H-pyrrole-2,5-dione) (M1)**

The general procedure was carried out using maleic anhydride (14.27 g, 146 mmol), 1,8-octanediamine (10.0 g, 69.3 mmol), sodium acetate (1.14 g, 13.9 mmol), and acetic anhydride (15.57 g, 153 mmol). The resulting compound was purified by column chromatography [98:2 DCM:ethyl acetate (EtOAc)], and the product was obtained as a white solid (5.2 g/25%):  $R_f$  (95:5 DCM:EtOAc) = 0.5; m.p. = 124.5  $^\circ\text{C}$ .

$^1\text{H}$  NMR (400 MHz, DMSO):  $\delta$  (ppm) = 6.99 (s, 4H), 3.37, (t, 4H,  $J$  = 6.7 Hz), 1.46 (m, 4H), 1.19 (m, 8H);  $^{13}\text{C}$  NMR (400 MHz, DMSO):  $\delta$  (ppm) = 171.54, 134.90, 37.47, 28.77, 28.32, 26.46; Electrospray MS (positive ion mode): calcd. for  $\text{C}_{16}\text{H}_{21}\text{N}_2\text{O}_4$  [ $\text{M} + \text{H}$ ] $^+$ :  $m/z$  = 305.15; found: 305.2, calcd. for  $\text{C}_{16}\text{H}_{20}\text{N}_2\text{O}_4\text{Na}$  [ $\text{M} + \text{Na}$ ] $^+$ :  $m/z$  = 327.14; found: 327.2.

**1,1'-(Cyclohexane-1,3-diylbis(methylene))bis(1H-pyrrole-2,5-dione) (M2)**

The general procedure was carried out using maleic anhydride (20.59 g, 210 mmol), 1,3-cyclohexanebis(methylamine) (14.22 g, 100 mmol), sodium acetate (1.64 g, 20 mmol), and acetic anhydride (22.46 g, 220 mmol). The resulting compound was purified by column chromatography (98:2 DCM:EtOAc), and the product was obtained as a white solid (3.55 g/12%):  $R_f$  (95:5 DCM:EtOAc) = 0.42; m.p. = 161.3  $^\circ\text{C}$ .

$^1\text{H}$  NMR (400 MHz, DMSO):  $\delta$  (ppm) = 6.97 (s, 4H), 3.19 (d, 4H,  $J$  = 6.7 Hz), 1.51 (m, 6H), 1.13 (m, 1H), 0.78 (m, 2H), 0.57 (m, 1H);  $^{13}\text{C}$  NMR (400 MHz, DMSO):  $\delta$  (ppm) = 171.68, 134.81, 43.59, 36.75, 34.59, 30.35, 25.00; Electrospray MS (positive ion mode): calcd. for  $\text{C}_{16}\text{H}_{20}\text{N}_2\text{O}_5$  [ $\text{M} + \text{H}_2\text{O}$ ] $^+$ :  $m/z$  = 320.15; found: 320.2, calcd. for  $\text{C}_{16}\text{H}_{18}\text{N}_2\text{O}_4\text{Na}$  [ $\text{M} + \text{Na}$ ] $^+$ :  $m/z$  = 325.11; found: 325.2, calcd. for  $\text{C}_{16}\text{H}_{18}\text{N}_2\text{O}_4\text{K}$  [ $\text{M} + \text{K}$ ] $^+$ :  $m/z$  = 341.23; found: 341.2.

**1,1'-(1,3-Phenylenebis(methylene))bis(1H-pyrrole-2,5-dione) (M3)**

The general procedure was carried out using maleic anhydride (20.59 g, 210 mmol), *m*-xylylenediamine (13.62 g, 100 mmol), sodium acetate (1.64 g, 20 mmol), and acetic anhydride (22.46 g, 220 mmol). The resulting compound was purified by column chromatography (97:3 DCM:EtOAc), and the product was obtained as a white solid (6.51 g/22%):  $R_f$  (95:5 DCM:EtOAc) = 0.35; m.p. = 129.8  $^\circ\text{C}$ .

$^1\text{H}$  NMR (400 MHz, DMSO):  $\delta$  (ppm) = 7.28 (t, 1H,  $J$  = 0.2 Hz), 7.11 (m, 3H), 7.09 (s, 4H), 4.56 (s, 4H);  $^{13}\text{C}$  NMR (400 MHz, DMSO):  $\delta$  (ppm) = 171.25, 137.58, 135.16, 129.34, 126.69, 126.44; Electrospray MS (positive ion mode): calcd. for  $\text{C}_{16}\text{H}_{12}\text{N}_2\text{O}_4\text{Na}$  [ $\text{M} + \text{Na}$ ] $^+$ :  $m/z$  = 319.27; found: 319.1.

**1,1'-((Ethane-1,2-diylbis(oxy))bis(ethane-2,1-diyl))bis(1H-pyrrole-2,5-dione) (M4)**

The general procedure was carried out using maleic anhydride (13.23 g, 135 mmol), 2,2'-(ethylenedioxy)bis(ethylamine) (10.0 g, 67.5 mmol), sodium acetate (1.11 g, 13.5 mmol), and acetic anhydride (15.15 g, 148 mmol). The resulting compound was purified by column chromatography (95:5 DCM:EtOAc), and the product was obtained as a white solid (4.5 g/22%):  $R_f$  (80:20 DCM:EtOAc) = 0.35; m.p. = 98.05  $^\circ\text{C}$ .

$^1\text{H}$  NMR (400 MHz, DMSO):  $\delta$  (ppm) = 7.01 (s, 4H), 3.53 (m, 4H), 3.47 (m, 4H), 3.42 (s, 4H);  $^{13}\text{C}$  NMR (400 MHz, DMSO):  $\delta$  (ppm) = 171.5, 134.9, 69.76, 67.42, 37.24; Electrospray MS (positive ion mode): calcd. for  $\text{C}_{14}\text{H}_{17}\text{N}_2\text{O}_6$  [ $\text{M} + \text{H}$ ] $^+$ :  $m/z$  = 309.11; found: 309.1, calcd. for  $\text{C}_{16}\text{H}_{20}\text{N}_2\text{O}_4\text{Na}$  [ $\text{M} + \text{Na}$ ] $^+$ :  $m/z$  = 331.10; found: 331.0.

**General Procedure for Synthesis of Bisfurans**

To a 500-mL round-bottomed flask equipped with a magnetic stir bar, 1,8-octanediamine (47.9 equiv), triethylamine (95.7 equiv), dimethylaminopyridine (DMAP, 1 equiv), and DCM (200 mL) were added. The solution was chilled on ice, and then furoyl chloride (100 equiv) in DCM (50 mL) was

added dropwise. The ice bath was removed, and the mixture was stirred at room temperature overnight. The organic layer was extracted with NaHCO<sub>3</sub> (5 × 100 mL) and dried over MgSO<sub>4</sub>, and then the solvent was removed under vacuum. The resulting compounds were purified by column chromatography.

#### *N,N'*-(Octane-1,8-diyl)bis(furan-2-carboxamide) (F1)

The general procedure was carried out using 1,8-octanediamine (10.0 g, 69.3 mmol), triethylamine (14.2 g, 141 mmol), DMAP (0.17 g, 1.35 mmol), and furoyl chloride (19.0 g, 146 mmol). The resulting compound was purified by column chromatography (98:2 DCM:EtOAc), and the product was obtained as a white solid (21.5 g/92%): *R*<sub>f</sub> (50:50 DCM:EtOAc) = 0.29; m.p. = 135.3 °C.

<sup>1</sup>H NMR (400 MHz, DMSO): δ (ppm) = 8.30 (t, 2H, *J* = 5.7 Hz), 7.80 (d, 2H, *J* = 1.0 Hz), 7.05 (d, 2H, *J* = 3.4 Hz), 6.60 (dd, 2H, *J* = 1.7 Hz), 3.18 (q, 4H, *J* = 6.7 Hz), 1.48 (m, 4H), 1.27 (m, 8H); <sup>13</sup>C NMR (400 MHz, DMSO): δ (ppm) = 158.09, 148.61, 145.17, 113.39, 112.18, 38.87, 29.62, 29.17, 26.16; Electrospray MS (positive ion mode): calcd. for C<sub>18</sub>H<sub>24</sub>N<sub>2</sub>O<sub>4</sub>Na [M + Na]<sup>+</sup>: *m/z* = 355.38; found: 355.16.

#### *N,N'*-(Cyclohexane-1,3-diylbis(methylene))bis(furan-2-carboxamide) (F2)

The general procedure was carried out using 1,3-cyclohexanedibis(methylamine) (10.0 g, 70.3 mmol), triethylamine (14.2 g, 141 mmol), DMAP (0.17 g, 1.41 mmol), and furoyl chloride (19.0 g, 146 mmol). The resulting compound was purified by column chromatography (95:5 DCM:EtOAc), and the product was obtained as a white solid (3.5 g/15%): *R*<sub>f</sub> (50:50 DCM:EtOAc) = 0.23; m.p. = 204.3 °C.

<sup>1</sup>H NMR (400 MHz, DMSO): δ (ppm) = 8.30 (t, 2H, *J* = 5.3 Hz), 7.80 (d, 2H, *J* = 3.7 Hz), 7.05 (d, 2H, *J* = 3.4 Hz), 6.60 (dd, 2H, *J* = 1.7 Hz), 3.04 (t, 4H, *J* = 5.3 Hz), 1.70 (m, 4H), 1.51 (m, 2H), 1.18 (m, 1H), 0.80 (m, 2H), 0.55 (m, 1H); <sup>13</sup>C NMR (400 MHz, DMSO): δ (ppm) = 158.23, 148.56, 145.18, 113.45, 112.17, 45.30, 37.83, 35.37, 30.95, 25.50; Electrospray MS (positive ion mode): calcd. for C<sub>18</sub>H<sub>23</sub>N<sub>2</sub>O<sub>4</sub> [M + H]<sup>+</sup>: *m/z* = 331.39; found: 331.2.

#### *N,N'*-(1,3-Phenylenebis(methylene))bis(furan-2-carboxamide) (F3)

The general procedure was carried out using *m*-xylylenediamine (10.0 g, 73.4 mmol), triethylamine (14.9 g, 147 mmol), DMAP (0.17 g, 1.41 mmol), and furoyl chloride (20.13 g, 154 mmol). The resulting compound was purified by column chromatography (95:5 DCM:EtOAc), and the product was obtained as a white solid (21.8 g/92%): *R*<sub>f</sub> (50:50 DCM:EtOAc) = 0.27; m.p. = 181.8 °C.

<sup>1</sup>H NMR (400 MHz, DMSO): δ (ppm) = 8.88 (t, 2H, *J* = 6.1 Hz), 7.82 (d, 2H, *J* = 1.2 Hz), 7.1–7.3 (m, 6H), 6.61 (dd, 2H, *J* = 1.7 Hz), 4.39 (d, 4H, *J* = 6.2 Hz); <sup>13</sup>C NMR (400 MHz, DMSO): δ (ppm) = 158.20, 148.33, 145.47, 140.05, 128.72, 126.62, 126.28, 113.88, 112.27, 42.33; Electrospray MS (positive ion mode): calcd. for C<sub>18</sub>H<sub>16</sub>N<sub>2</sub>O<sub>4</sub> [M + H]<sup>+</sup>: *m/z* = 325.04; found:

325.1, calcd. for C<sub>16</sub>H<sub>20</sub>N<sub>2</sub>O<sub>4</sub>Na [M + Na]<sup>+</sup>: *m/z* = 347.32; found: 347.1.

#### *N,N'*-(Ethane-1,2-diylbis(oxy))bis(ethane-2,1-diyl)bis(furan-2-carboxamide) (F4)

The general procedure was carried out using 2,2'-(ethylene-dioxy)bis(ethylamine) (10.0 g, 67.5 mmol), triethylamine (13.66 g, 135 mmol), DMAP (0.17 g, 1.41 mmol), and furoyl chloride (18.5 g, 142 mmol). The resulting compound was purified by column chromatography (95:5 DCM:EtOAc), and the product was obtained as a white solid (10.9 g/48%): *R*<sub>f</sub> (95:5 DCM:MeOH) = 0.33; m.p. = 72.4 °C.

<sup>1</sup>H NMR (400 MHz, DMSO): δ (ppm) = 8.30 (t, 2H, *J* = 5.5 Hz), 7.80 (d, 2H, *J* = 0.9 Hz), 7.08 (d, 2H, *J* = 3.3 Hz), 6.60 (dd, 2H, *J* = 1.7 Hz), 3.55 (s, 4H), 3.49 (m, 4H), 3.35 (m, 4H); <sup>13</sup>C NMR (400 MHz, DMSO): δ (ppm) = 158.28, 148.36, 145.36, 113.71, 112.24, 69.97, 69.31, 38.81; Electrospray MS (positive ion mode): calcd. for C<sub>16</sub>H<sub>20</sub>N<sub>2</sub>O<sub>4</sub>Na [M + Na]<sup>+</sup>: *m/z* = 359.33; found: 359.1.

#### Mixture Preparation

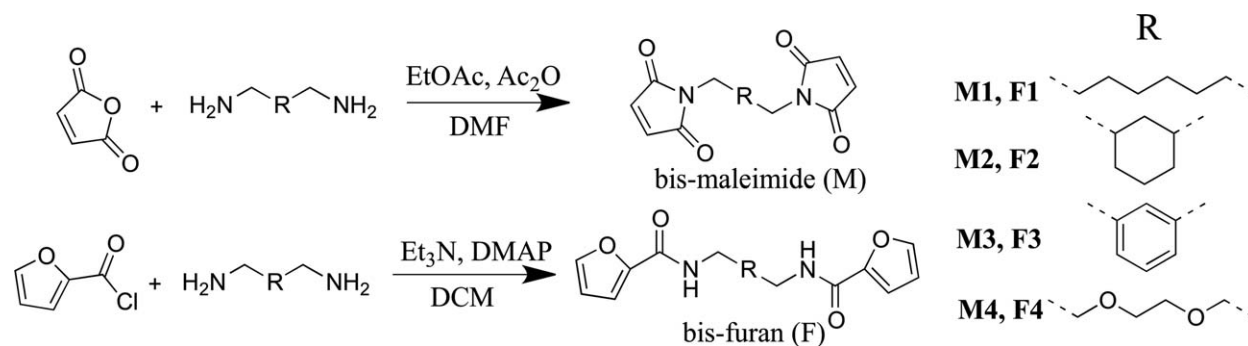
In a typical example, equimolar amounts of bismaleimide and bisfuran were combined in a vial. DCM/MeOH (95:5 v/v, 5 mL) was then added, and the vial was shaken to ensure complete dissolution. The solvent was then removed under vacuum, and the resulting solid mixture was ground into a uniform powder.

#### Nanoindentation

Samples were prepared by transferring the powder mixture (~50 mg) to a steel sample disc (15 mm diameter). The disc was placed on a hotplate that was preheated ~20 °C above the melting point of the mixture. Air bubbles that appeared during melting were removed by agitation of the liquid with a clean spatula. The sample discs were removed from the heat source and stored at 60 °C, resulting in smooth films with relatively flat surfaces. Samples were allowed to equilibrate at room temperature for 1 h before measurements were made. A 10-2-10 load function was used (10-s load time, 2-s hold, and 10-s unload time) with a maximum load of 1000 μN. Longer hold times have been claimed to be more effective for nanoindentation of viscoelastic materials.<sup>31</sup> A hold time of 30 s was also attempted; however, results for modulus and hardness were largely similar, and this often resulted in adhesion of compliant material to the indenter tip, which significantly affected subsequent measurements. Measurements were made in 3 × 3 grids, with a spacing of 15 μm between each indentation. Three separate locations spaced at least 1 mm apart were used on each sample stub. Values reported represent an average of these 27 measurements. Control samples [poly(methyl methacrylate) and quartz] were measured before and after each set of measurements to ensure that measurements were within 5% of their expected values.

#### <sup>1</sup>H NMR Kinetics

Solid films were stored at 60 °C for the specified period of time and then dissolved in the NMR solvent. Reversion to



**SCHEME 1** Synthetic pathway of bismaleimides and bisfurans.

furan/maleimide was accomplished by melting 10 mg of the neat sample in an NMR tube and then immediately quenching in liquid nitrogen. The resulting solid was then dissolved in the NMR solvent.

### DSC Kinetics

Separate samples were prepared for each designated aging time. Samples were weighed and crimped in aluminum DSC pans and subjected to a heat/cool/heat cycle. The pans were then stored at 60 °C for the specified period of time and then subjected to another heat/cool/heat cycle.

### Adhesion Testing

Two 3/8"-diameter dowels made of stainless steel (Grade 303) were preheated ~20 °C above the melting point of the monomer mixture. The powdered mixture ( $5 \pm 0.5$  mg), which had been compressed into pellet form for easier handling, was then carefully placed on the polished surface of the dowel. The solid completely melted within seconds, and an alignment sleeve was then slipped over the first dowel, and a second dowel placed in the tube onto the surface of the molten sample, applying minimal downward pressure. The sleeve was bored to allow 0.002" clearance to ensure perfect alignment of the two dowels. The top dowel was turned gently for three complete revolutions to ensure complete surface area coverage at the interface of the two dowels. Only the weight of the upper dowel ( $30.38 \pm 0.03$  g) was used to compress the liquid samples. The samples were incubated at 60 °C for 4 days and then equilibrated at room temperature for 1 h prior to testing for tensile strength. Eight samples were prepared for each test. Samples were tested on an Instron 3367 at an extension rate of 100  $\mu\text{m}/\text{min}$  until complete fracture had occurred. The highest and lowest values were eliminated, and

the results for breaking strength were reported as an average of the six remaining measurements.

### RESULTS AND DISCUSSION

Four pairs of bismaleimides and bisfurans, varying only in their linking chemistry, were prepared and characterized. Four different diamines, including *n*-octyl, 1,3-dimethylcyclohexyl, 1,3-dimethylphenyl, and 1,2-dimethoxyethane, were used as starting materials such that the spacer chain between the two functional groups contained approximately the same number of atoms (Scheme 1). The bismaleimides were prepared by condensation of two equivalents of maleic anhydride with the diamine using sodium acetate and acetic anhydride. The bisfurans were prepared using the same series of diamines coupled with two equivalents of furfuryl chloride. Therefore, the bisfurans had amide linkages to the furan rings, thus their spacer groups were somewhat different from those of the bismaleimides. Nonetheless, the spacer chains within each of the bisfuran and bismaleimide series were consistent, and the resulting monomers therefore represented a series having linear alkyl, dimethylcyclohexyl, dimethylphenyl, and ethylenedioxy linkages (Scheme 1).

Each of the eight compounds was characterized by DSC to determine their melting and crystallization transitions. For each compound, sharp melting peaks were observed that spanned a wide temperature range, commensurate with the substantial differences in chemistries of the four spacer groups (Table 1). Crystallization peaks were observed on the cooling cycle only for compounds **M1, F1** and **M2, F2**, consistent with the difference in crystallinity of the four spacer groups.

Complete dissolution of equimolar amounts of bismaleimide and bisfuran in DCM/MeOH (95:5 vol %) ensured intimate

**TABLE 1** Melting Point and Crystallization Point of Bismaleimides and Bisfurans

Bismaleimides			Bisfurans		
Compound	Melting Point (°C)	Crystallization Point (°C)	Compound	Melting Point (°C)	Crystallization Point (°C)
<b>M1</b>	124.5	91.8	<b>F1</b>	135.3	93.2
<b>M2</b>	161.3	144.3	<b>F2</b>	204.3	167.0
<b>M3</b>	129.8	–	<b>F3</b>	181.8	–
<b>M4</b>	98.1	–	<b>F4</b>	72.4	–

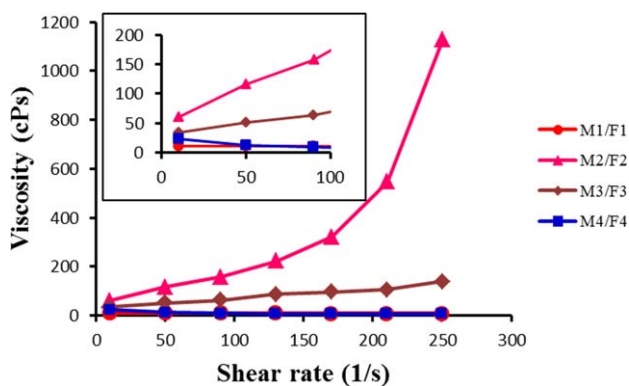


**FIGURE 3** Viscosities of molten M/F mixtures: **M1/F1** measured at 120 °C, **M2/F2** measured at 190 °C, **M3/F3** measured at 150 °C, and **M4/F4** measured at 90 °C. Inset shows magnified scale at low shear rates. [Color figure can be viewed in the online issue, which is available at [wileyonlinelibrary.com](http://wileyonlinelibrary.com).]

mixing of the two compounds. Solvent removal under reduced pressure resulted in white solids, which were then ground into powders. In all cases,  $^1\text{H}$  NMR spectroscopy confirmed that the mixtures consisted of two discrete compounds, with no extraneous peaks indicative of DA coupling. Comparison of integration values of the signals corresponding to the  $\alpha$ -vinyl protons of the furan and the two equivalent maleimide vinyl protons (at 7.8 and 7.0 ppm,

respectively) confirmed that the two compounds were present in a 1:1 equimolar ratio.

The powdered mixtures were heated until complete melting had occurred. Viscosities of the molten mixtures were well below 100 cPs, making them easily manageable for all forms of material processing (Fig. 3).<sup>32</sup> The apparent dilatant behavior of the two mixtures **M2/F2** and **M3/F3** was attributed to the higher temperature required for melting, which may have resulted in irreversible crosslinking of the maleimide resins during the course of the measurement.<sup>33</sup> To minimize the degree of crosslinking, the molten samples were removed from the heat source within 10–15 s of melting and cooled to 60 °C, resulting in the formation of clear tacky resins which, on standing, turned to hard solid films. Interestingly, **M1/F1** and **M4/F4** remained tacky for several hours after cooling, whereas **M2/F2** and **M3/F3** turned to clear, hard solid films immediately on removal of the heat source. Furthermore, **M1/F1** became completely opaque on cooling, whereas **M2/F2**, **M3/F3**, and **M4/F4** remained as clear films indefinitely (Fig. 4). The opacity observed in **M1/F1** was attributed to the crystalline nature of the linear alkyl chains, and indeed XRD analysis revealed a significant degree of crystallinity in the **M1/F1** mixture, whereas the other three mixtures were found to be amorphous (Fig. 5). Control experiments, in which the components **M1–M4** and **F1–F4** were melted individually, yielded either sticky films that did not harden with time or crystalline solids with no film-forming capacity.



**FIGURE 4** Polymer films cast from molten mixtures: (a) **M1/F1**, (b) **M2/F2**, (c) **M3/F3**, and (d) **M4/F4**. [Color figure can be viewed in the online issue, which is available at [wileyonlinelibrary.com](http://wileyonlinelibrary.com).]

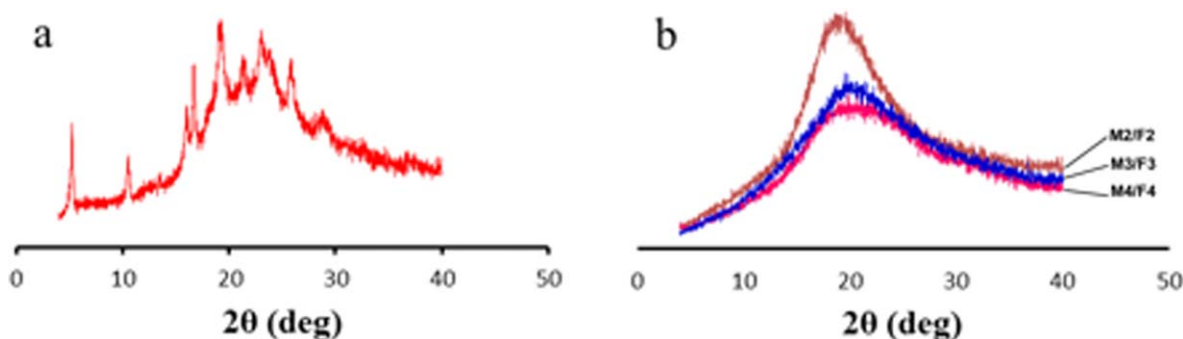


**FIGURE 5** X-ray diffraction data for polymerized materials: (a) **M1/F1** mixture and (b) **M2/F2** (brown), **M3/F3** (pink), and **M4/F4** (blue) mixtures. [Color figure can be viewed in the online issue, which is available at [wileyonlinelibrary.com](http://wileyonlinelibrary.com).]

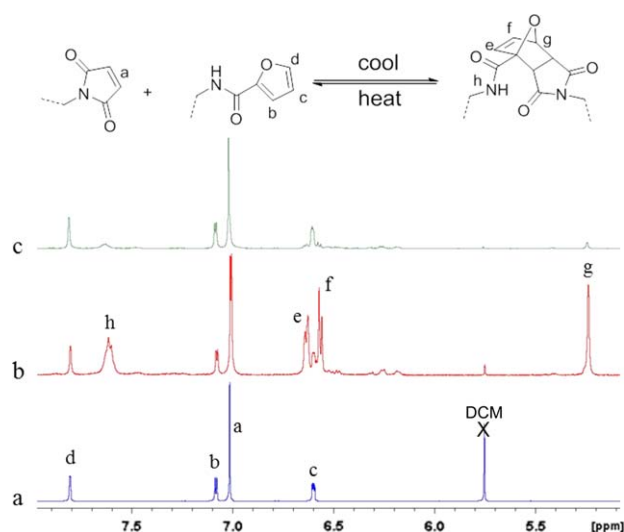


**FIGURE 6**  $^1\text{H}$  NMR showing the reversible polymerization of **M4/F4**. Spectra were recorded prior to melting (a), after melting and incubation at  $60^\circ\text{C}$  for 7 days (b), and after remelting and rapid quenching in liquid nitrogen (c). Similar data for the other mixtures can be found in Supporting Information Figures S1–S3. [Color figure can be viewed in the online issue, which is available at [wileyonlinelibrary.com](http://wileyonlinelibrary.com).]

$^1\text{H}$  NMR spectroscopy confirmed that reversible DA coupling of the furan and maleimide moieties had occurred (Fig. 6 and Supporting Information Figs. S1–S3). Figure 6(a) shows the spectrum for the unheated mixture of the two powdered components **M4** and **F4** in an equimolar ratio. All peak assignments and integrations corresponded to the peaks observed in the spectra of the individual components, confirming that coupling had not occurred between the two compounds prior to heating. After a single melt/cool cycle, the resulting solid film was stored for 7 days at  $60^\circ\text{C}$ . The spectrum of the resulting material was consistent with the formation of a DA adduct [Fig. 6(b)]. Specifically, a new peak, attributed to the bridgehead proton on the newly formed fused ring system, emerged at 5.2 ppm. Furthermore, the appearance of a doublet of doublets centered at 6.6 ppm could be attributed to the new norbornyl double bond. These new signals increased in intensity in a 2:1 ratio, consistent with the number of protons generating the signals. Two additional signals would be expected from the protons at the junction of the two fused rings; however, these peaks were obscured in the aliphatic region of the spectrum. Melting of the solid film, followed by a rapid quench in liquid nitrogen, almost completely restored the original spectrum [Fig. 6(c)], thus confirming the reversibility of the reaction. It should be noted that the signal at 7.8 ppm did not quantitatively disappear during the incubation period, indicating that the DA polymerization did not go to completion. Kinetic studies were therefore undertaken for each of the four mixtures to quantify the degree of polymerization in each case.

Molten mixtures were cooled and stored at  $60^\circ\text{C}$  as described above, and  $^1\text{H}$  NMR spectra were acquired at spe-

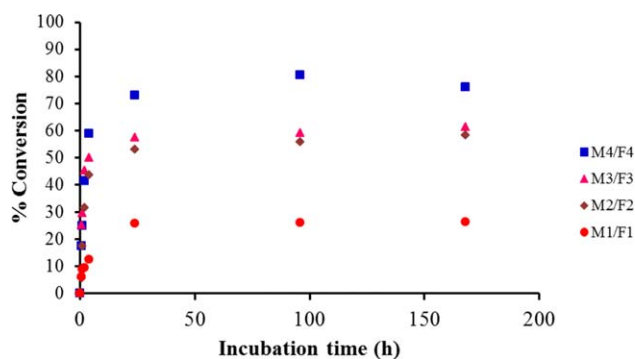


**FIGURE 7** Polymer conversion percentages over time, determined by  $^1\text{H}$  NMR spectroscopy. [Color figure can be viewed in the online issue, which is available at [wileyonlinelibrary.com](http://wileyonlinelibrary.com).]

cific time intervals. The ratio of the newly formed product peak at 5.2 ppm to the original vinyl furan peak at 7.8 ppm served as an indicator of polymer conversion, which was calculated using the formula  $i_{5.2}/(i_{5.2} + i_{7.8}) \times 100\%$ , where  $i_x$  is the integral of the NMR peak at  $x$  ppm. Mixtures **M1/F1** and **M4/F4**, although having similarly slow hardening times, had significantly different polymer conversion percentages, the former having a much lower value (Fig. 7). It is believed that the inherent crystallinity in **M1/F1** restricted mobility of the maleimide and furan moieties in the cooled film, thus suppressing more extensive DA coupling. Despite its slow hardening rate, the **M4/F4** mixture exhibited the fastest and most extensive polymerization, presumably enabled by the flexibility of the diether linkers.

Thermal analysis was performed on both the monomeric powder mixtures and the solidified polymers and provided further evidence for polymerization (Fig. 8). Initial heating of the maleimide and furan powders produced a sharp melting peak. A second heating of the mixture immediately following the cooling cycle resulted in the disappearance of this peak and the appearance of a very weak, broad, and endothermic peak corresponding to the cleavage (retro-DA reaction) of a small number of DA linkages that were formed in the short duration of sample cooling. After the initial heat/cool/heat cycle was completed, samples were cooled and stored at  $60^\circ\text{C}$ , and the heat/cool/heat cycle was repeated after 1, 4, and 7 days. On first heating of the incubated samples, two endothermic transitions were observed at about 100 and  $135^\circ\text{C}$  representing, respectively, the collapse of the endo and exo stereoisomers of the DA linkages within the polymer via the retro-DA reaction. At 24 h of incubation, the size of the two new peaks was significant, commensurate with the growth of the polymer during that time. In each case, a second heating (dashed line) resulted in the single broad endothermic peak observed in the initial heat/cool/heat cycle, corresponding to the formation and cleavage of only the exo DA linkages. Peak intensities did not change substantially after 24 h of aging, confirming that polymer conversion was maximized after 24 hours, which is consistent with the observed NMR data (above). Interestingly, the peak at lower temperature diminished in size after 7 days of incubation.

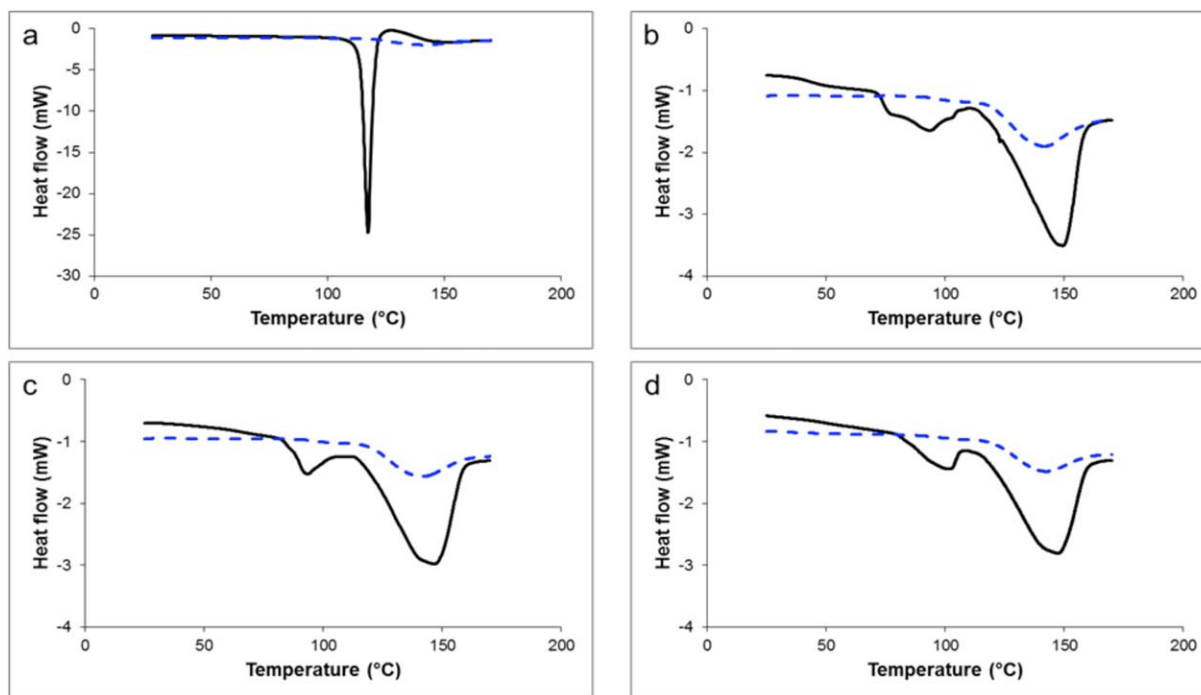


**FIGURE 8** DSC cycling of the **M1/F1** mixture. Initial heating (solid line), second heating, and immediately following first (dashed line): (a) dry blended mixture of the monomers; (b) 24 hours after initial heat/cool/heat cycle; (c) 4 days after initial heat/cool/heat cycle; and (d) 7 days after initial heat/cool/heat cycle. DSC traces for all mixtures can be found in Supporting Information Figures S4–S7. [Color figure can be viewed in the online issue, which is available at [wileyonlinelibrary.com](http://wileyonlinelibrary.com).]

It is believed that this is due to a slow isomerization of the endo form of the DA adduct to the more thermodynamically stable exo form.<sup>29</sup> The appearance of only a single peak at about 135 °C for the polymer **M4/F4**, regardless of incubation time, is attributed to the long solidification times of the resulting polymer, which led to the formation of only the more thermodynamically stable isomer.<sup>29</sup> A glass transition would also be expected to appear in each trace; however, this was only observed for the polymer **M4/F4** at about 65 °C. It is believed that the glass transitions for the polymers having more rigid spacers occurred at higher temperatures and were thus obscured by the two broad peaks arising from the retro-DA reaction.

Rheology of the films was measured using a Hysitron® nanoindenter. The inherent brittleness of the polymers precluded sample preparation for conventional DMA analysis, thus rheology of the films was determined using nanoindentation. This technique is commonly used to determine rheological characteristics of a wide variety of materials.<sup>34–36</sup> An indenter tip with well-known geometry is used to penetrate a sample film under load-controlled conditions. The depth of penetration can be used to calculate the exact area of indentation, which in turn allows for calculation of the hardness ( $H$ ) of the material, as the maximum load over the area of penetration. A plot of the load versus displacement of the tip during indentation can be recorded, and the stiffness and reduced modulus ( $E_r$ ) of the material can be calculated from the unloading curve. This allows for rheological measure-

ments of samples in their working state; measurements can be made on thin films cast by simple melting and cooling of the small molecule mixtures. Samples were prepared by melting the powdered mixtures on a 15-mm-diameter metal disc. Measurements were made directly on the films after aging for 4 days at 60 °C on three remote spots on each disc in  $3 \times 3$  grids with a spacing of 15  $\mu\text{m}$  between each indent. A load of 1000  $\mu\text{N}$  with a 10-s loading time, 2-s hold time, and 10-s unloading time (10-2-10 load function) was used. Modulus and hardness data for the four sets of compounds, averaged from the 27 separate indentation measurements made for each compound, are provided in Figure 9.

Hardness data indicated that **M1/F1** was dramatically softer than the other three mixtures, although this did not seem to be the case macroscopically. The **M1/F1** samples exhibited a much higher degree of macroroughness on the crystalline surface, making them difficult to measure by nanoindentation. Furthermore, they were significantly more brittle than the other three polymers and had a decidedly lower level of adhesion to metal, often resulting in complete delamination of the films from the metal support stubs. It is therefore conceivable that some degree of delamination had occurred on the samples being measured, which would profoundly influence the nanoindentation measurement. This is supported by the images in Figure 10, which depict micrographs of the indents made in each sample. The nine indents made in the **M1/F1** sample are not observed, whereas they are clearly visible in the other samples. This could be attributed to

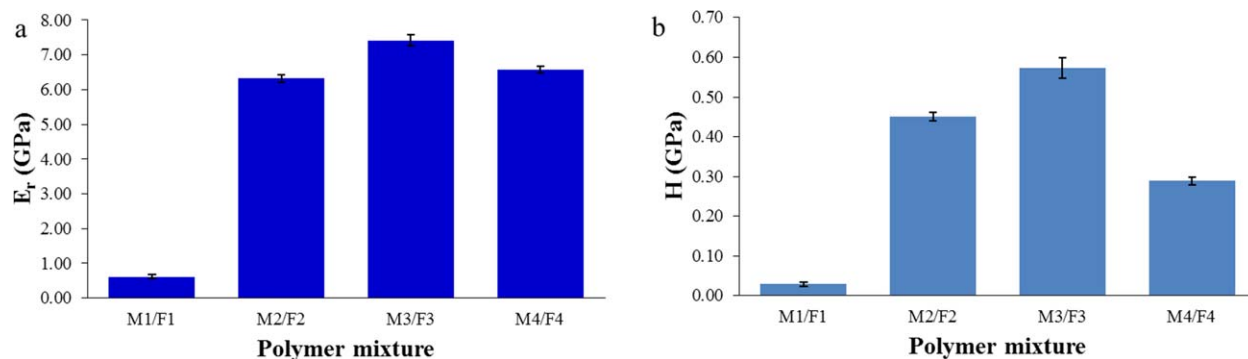


**FIGURE 9** Rheological data of polymer films measured by nanoindentation: (a) reduced modulus and (b) hardness. [Color figure can be viewed in the online issue, which is available at [wileyonlinelibrary.com](http://wileyonlinelibrary.com).]

elastic response of the material to the indents or to microdelamination, resulting in a lack of compression of the film by the nanoindenter tip. Attempts to bond the film to the metal support stub using epoxy resins did not influence the data.

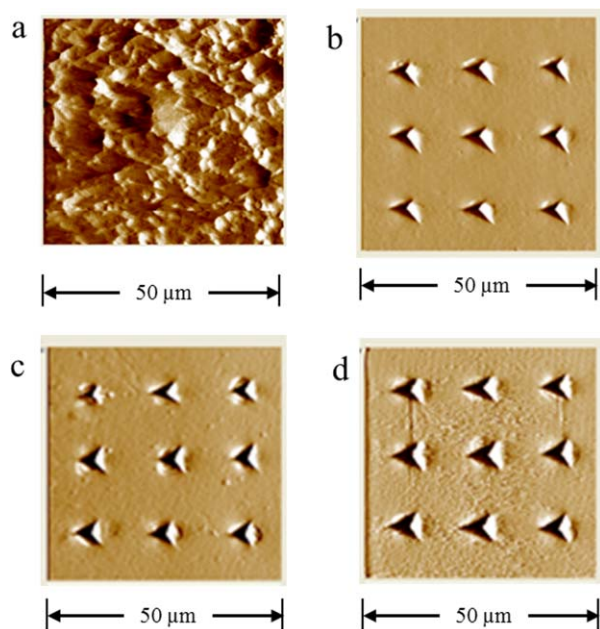


**FIGURE 10** Micrographs showing typical  $3 \times 3$  nanoindentation grids for (a) **M1/F1**; (b) **M2/F2**; (c) **M3/F3**; and (d) **M4/F4**. [Color figure can be viewed in the online issue, which is available at [wileyonlinelibrary.com](http://wileyonlinelibrary.com).]

Hardness and modulus of the polymer films could not be directly correlated to the rate or conversion data reported in Figure 7. Although **M4/F4** produced the highest polymer conversion rate, it was not the hardest of the films measured. Thus, it appears that both the rigidity of the spacer chain and % polymer conversion play a role in the hardness of the polymer film. Kinetic data of the rheology of the films could not be determined for the first 24 h of curing as the initial samples were too soft for measurement by nanoindentation.

The mixture **M4/F4** afforded polymers having excellent film-forming characteristics, but required a long time to harden, and was ultimately found to be softer than either of the other film formers **M2/F2** and **M3/F3**. We therefore decided to explore the effects of combining the **M4/F4** monomer mixture with **M1/F1**, **M2/F2**, and **M3/F3** to potentially capture the advantages of both materials in each combination. Mixtures containing the maleimide/furan couples in 4:1, 1:1, and 1:4 ratios were prepared, and the polymer films were cast for rheological evaluation. The mixture **M4/F4** + **M1/F1** in a 4:1 ratio afforded a film that remained smooth and transparent after several weeks, thus demonstrating that the crystalline and amorphous materials could be combined to provide clear, hard films (Fig. 11). Higher loadings of the crystalline **M1/F1** resulted in rough, opaque films, similar to the **M1/F1** mixture itself. Nevertheless, a clear trend in hardness and modulus data could be observed for a series of mixtures of the two monomer pairs (Fig. 12). Combination of



**FIGURE 11** Polymer films cast from molten mixtures of **M4/F4** and **M1/F1** in ratios of (a) 0:100; (b) 20:80; (c) 50:50; (d) 80:20; and (e) 100:0. [Color figure can be viewed in the online issue, which is available at [wileyonlinelibrary.com](http://wileyonlinelibrary.com).]

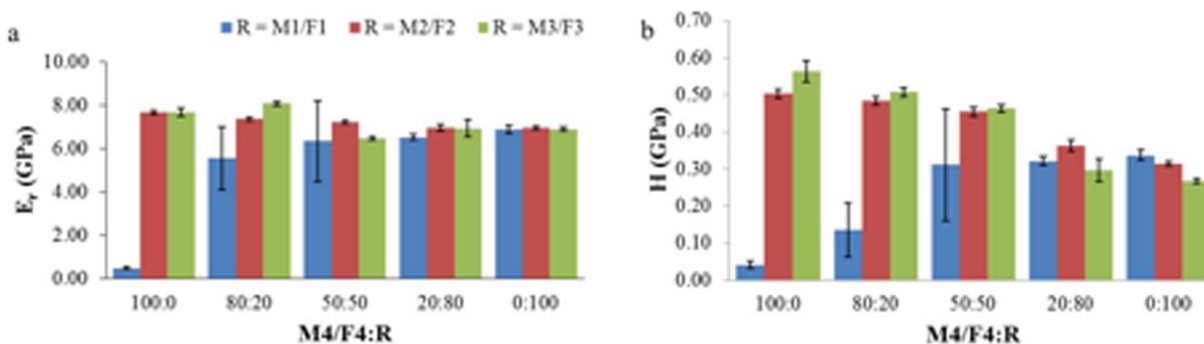


**FIGURE 12** Rheological data of polymer films measured by nanoindentation: (a) reduced modulus and (b) hardness. [Color figure can be viewed in the online issue, which is available at [wileyonlinelibrary.com](http://wileyonlinelibrary.com).]

**M4/F4** with the cyclohexyl-spaced monomers **M2/F2** yielded smooth, transparent films also having a clear trend in rheological characteristics. Hardness values were found to increase with increasing loading of the harder **M2/F2** monomers, whereas solidification times, noted by an audible click when the polymer films were tapped with a spatula, decreased with an increased loading of **M2/F2**. Similar observations were made with the combination of **M4/F4** and **M3/F3** (Fig. 12). Combination of the two mixtures therefore resulted in harder films while retaining the film-forming characteristics of the softer material, which was the intended result.

Although the polymers prepared in this study were found to be brittle, they also demonstrated a very high level of adhesion to the steel nanoindentation support stubs. We attempted to quantify the adhesion using a technique based on the American Society for Testing and Materials (ASTM) Method D2095,<sup>37</sup> used for measuring the tensile strength of adhesives. A controlled amount of each mixture was melted between two preheated stainless steel dowels, and, after cooling, tested for tensile adhesive strength (for images of the test apparatus, see Supporting Information Fig. S10). The brittleness and lack of adhesion to the nanoindentation sample stubs were in evidence here as the **M1/F1** mixtures completely failed on handling of the dowels after they had

cooled to room temperature. Furthermore, the brittle polymers **M2/F2** and **M3/F3** had lower adhesive strength than the more flexible **M4/F4**. It is significant that all three of these materials showed considerably higher adhesion than a typical film-forming polymer such as polyethylene glycol (PEG,  $M_n = 14,000$ ; Fig. 13). Although brittleness and wettability would be expected to play a key role in adhesion, the adhesion data for the reversible polymers also correlated well to the degree of polymerization discussed earlier (Fig. 7). It is therefore difficult to determine the most significant factor affecting adhesive strength, although we have demonstrated that adhesive strength is strongly influenced by spacer chemistry.

In keeping with our experiments combining the most elastic with the hardest materials for rheological evaluation (Fig. 12), we tested the adhesive strength of the combination **M4/F4** and **M3/F3**. Mixtures composed of 50:50 and 80:20 **M4/F4:M3/F3** were prepared and characterized using the same tensile test described above. As was found with the rheological properties of the polymer mixtures (Fig. 14), a trend could be observed from the stronger (**M4/F4**) to the weaker (**M3/F3**) adhesive. Interestingly, we did not find that the adhesion strength of the polymer was improved by any mixture of **M4/F4:M3/F3**, with the best adhesion coming from the **M4/F4** sample alone.

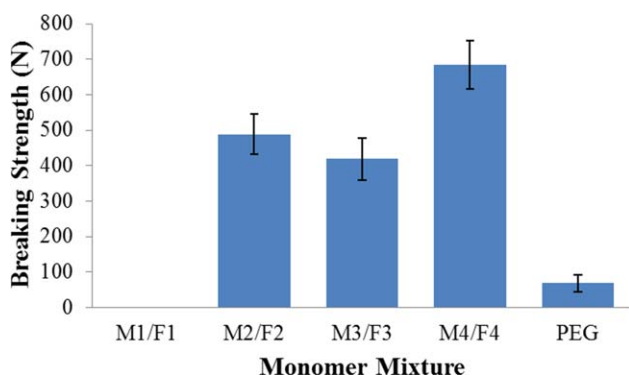


**FIGURE 13** Breaking strength of polymer mixtures. [Color figure can be viewed in the online issue, which is available at [wileyonlinelibrary.com](http://wileyonlinelibrary.com).]

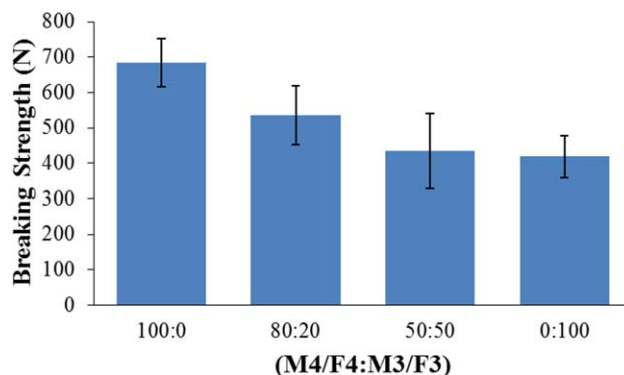


**FIGURE 14** Breaking strength of polymer mixtures composed of **M4/F4** and **M3/F3**. [Color figure can be viewed in the online issue, which is available at [wileyonlinelibrary.com](http://wileyonlinelibrary.com).]

## CONCLUSIONS

Linear reversible polymers, based on maleimide–furan DA linkages, have been prepared and characterized in monomeric and polymeric forms. Melting and cooling of equimolar amounts of a bismaleimide and bisfuran resulted in hard films with moduli and hardness ranging from 0.6 to 8 GPa and 0.1 to 0.6 GPa, respectively, as measured by nanoindentation. Solidification times of these films varied greatly, from seconds to hours. Differences in morphology were also observed, as the films ranged from opaque, crystalline solids to clear hard solids. Mixtures of the polymers having different spacer chemistries leveraged the advantages of both materials, resulting in rapidly solidified, hard materials with excellent film-forming characteristics. Adhesive strength was measured and found to be higher than a conventional film-forming polymer (PEG). Reversibility of the polymerization was verified by  $^1\text{H}$  NMR spectroscopy and DSC. Degree and rate of polymerization, as well as rheological properties and adhesion, were found to be dependent on the chemistry of the spacer molecule joining the functional end groups. Thus, this would provide a wide range of properties and working temperatures for polymer formation and processing.

## ACKNOWLEDGMENTS

This work was financially supported by the Xerox Research Centre of Canada. The authors thank Sonja Hadzidedic for completing numerous DSC analyses and for providing useful discussion.

## REFERENCES AND NOTES

- 1 Y. C. Yuan, T. Yin, M. Z. Rong, M. Q. Zhang, *Express Polym. Lett.* **2008**, *2*, 238–250.
- 2 S. D. Bergman, F. Wudl, *J. Mater. Chem.* **2008**, *18*, 41–62.
- 3 E. B. Murphy, F. Wudl, *Prog. Polym. Sci.* **2010**, *35*, 223–251.
- 4 D. Y. Wu, S. Meure, D. Solomon, *Prog. Polym. Sci.* **2008**, *33*, 479–522.
- 5 R. P. Wool, *Soft Matter* **2008**, *4*, 400–418.
- 6 T. A. Plaisted, S. Nemat-Nasser, *Acta Mater.* **2007**, *55*, 5684–5696.
- 7 Q. Tian, Y. C. Yuan, M. Z. Rong, M. Q. Zhang, *J. Mater. Chem.* **2009**, *19*, 1289–1296.
- 8 Y. L. Liu, C. Y. Hsieh, *J. Polym. Sci. Part A: Polym. Chem.* **2006**, *44*, 905–913.
- 9 X. X. Chen, F. Wudl, A. K. Mal, H. B. Shen, S. R. Nutt, *Macromolecules* **2003**, *36*, 1802–1807.
- 10 X. X. Chen, M. A. Dam, K. Ono, A. Mal, H. B. Shen, S. R. Nutt, K. Sheran, F. Wudl, *Science* **2002**, *295*, 1698–1702.
- 11 H. Laita, S. Boufi, A. Gandini, *Eur. Polym. J.* **1997**, *33*, 1203–1211.
- 12 K. Adachi, A. K. Achimuthu, Y. Chujo, *Macromolecules* **2004**, *37*, 9793–9797.
- 13 C. Gousse, A. Gandini, P. Hodge, *Macromolecules* **1998**, *31*, 314–321.
- 14 Y. Imai, H. Itoh, K. Naka, Y. Chujo, *Macromolecules* **2000**, *33*, 4343–4346.
- 15 Y. Zhang, A. A. Broekhuis, F. Picchioni, *Macromolecules* **2009**, *42*, 1906–1912.
- 16 H. Kwart, K. King, *Chem. Rev.* **1968**, *68*, 415–447.
- 17 E. B. Murphy, E. Bolanos, C. Schaffner-Hamann, F. Wudl, S. R. Nutt, M. L. Auad, *Macromolecules* **2008**, *41*, 5203–5209.
- 18 P. J. Boul, P. Reutenauer, J. M. Lehn, *Org. Lett.* **2005**, *7*, 15–18.
- 19 R. C. Boutelle, B. H. Northrop, *J. Org. Chem.* **2011**, *76*, 7994–8002.
- 20 J. W. Kamplain, C. W. Bielawski, *Chem. Commun.* **2006**, 1727–1729.
- 21 D. J. Coady, C. W. Bielawski, *Macromolecules* **2006**, *39*, 8895–8897.
- 22 C. Decker, C. Bianchi, S. Jonsson, *Polymer* **2004**, *45*, 5803–5811.
- 23 C. Decker, C. Bianchi, *Polym. Int.* **2003**, *52*, 722–732.
- 24 R. F. M. Lange, M. Van Gurp, E. W. Meijer, *J. Polym. Sci. Part A: Polym. Chem.* **1999**, *37*, 3657–3670.
- 25 F. H. Beijer, R. P. Sijbesma, H. Kooijman, A. L. Spek, E. W. Meijer, *J. Am. Chem. Soc.* **1998**, *120*, 6761–6769.
- 26 R. P. Sijbesma, F. H. Beijer, L. Brunsveld, B. J. B. Folmer, J. Hirschberg, R. F. M. Lange, J. K. L. Lowe, E. W. Meijer, *Science* **1997**, *278*, 1601–1604.
- 27 D. Montarnal, M. Capelot, F. Tournilhac, L. Leibler, *Science* **2011**, *334*, 965–968.
- 28 M. Watanabe, N. Yoshie, *Polymer* **2006**, *47*, 4946–4952.
- 29 J. Canadell, H. Fischer, G. de With, R. A. T. M. van Benthem, *J. Polym. Sci. Part A: Polym. Chem.* **2010**, *48*, 3456–3467.
- 30 A. Gandini, D. Coelho, A. J. D. Silvestre, *Eur. Polym. J.* **2008**, *44*, 4029–4036.
- 31 M. H. Nai, C. T. Lim, K. Y. Zeng, V. B. C. Tan, *J. Metastab. Nanocryst.* **2005**, *23*, 363–366.
- 32 A. Rochman, A. Frick, P. Martin, *Polym. Eng. Sci.* **2012**, *52*, 2114–2121.
- 33 B. A. Rozenberg, E. A. Dzhevadyan, R. Morgan, E. Shin, *Polym. Adv. Technol.* **2002**, *13*, 837–844.
- 34 M. R. Naimi-Jamal, G. Kaupp, *Macromol. Symp.* **2008**, *274*, 72–80.
- 35 W. C. Oliver, G. M. Pharr, *MRS Bull.* **2010**, *35*, 897–907.
- 36 G. M. Pharr, W. C. Oliver, *MRS Bull.* **1992**, *17*, 28–33.
- 37 ASTM-D2095. Standard Test Method for Tensile Strength of Adhesives by Means of Bar and Rod Specimens. American Society for Testing and Materials: West Conshohocken, Pennsylvania, **1996**.